Knowledge Empowerment Foundation
Empowering Knowledge
www.kemfo.org

EXPLORATORY MATERIALS SCIENCE RESEARCH

E-ISSN : 2582-8444

Original Research Article

EMSR, 1(1) 2020 [30-38]

Hydrothermal synthesis of titanate nanostructures as a high surface area adsorbent

Mohd Hasmizam Razali*, Nur Arifah Ismail, Khairul Anuar Mat Amin
Advanced Nanomaterials Research Group, Faculty of Science and Marine Environment, Universiti Malaysia Terengganu, 21030 Kuala Nerus, Terengganu, (MALAYSIA)
E-mail: mdhasmizam@umt.edu.my
DOI : https://dx.doi.org/10.47204/EMSR.1.1.2020.030-038

ABSTRACT

In this research, titanate nanostructures were prepared via a simply hydrothermal method with different hydrothermal temperature which are 100, 150, 200, 250 °C for 24 hours. Commercial TiO_2 powder (merck) was used as a precursor and the synthesized samples were characterized using FT-IR, XRD, FESEM, nitrogen gas adsorption and TG analyses. The results revealed that the structure, texture and morphology of samples strongly depend on the temperature of hydrothermal treatment. Hydrogen trititanate nanofibrous was produced at 150 °C, meanwhile, sodium trititanate nanorods were obtained at 200 and 250 °C. At low hydrothermal treatment (100 °C), no reaction was happening. The diameter of nanofibrous and nanorods were found to be (25-30) nm and (250-300) nm, respectively. Hydrogen trititanate nanofibrous possessed the highest surface area due to their small elongated fiber structures thus offers a great potential as adsorbent.

KEYWORDS

Hydrothermal; Titanate; Nanostructures; Adsorbent.

INTRODUCTION

In 1998, first researcher was successfully produce TiO_2 derived nanotubes by a simple hydrothermal treatment of TiO_2 powder in 10 M NaOH aqueous solution and subsequently washed with HCl aqueous solution[1]. This method is an inexpensive and simple method, and has recently been employed to fabricate titanate nanomaterials with various morphologies and diameters under different hydrothermal conditions. Later, many groups have tried to optimize the synthesis conditions to effectively prepare high-yield nanotubes from this simple and cost-effective technology[2-4]. This is because TiO_2 and/or titanate nanotubes derived from such a method are characterized by high specific surface area and pore volume, they may be a promising and important adsorbent for the removal of air pollutants. In addition, since TNT derived from hydrothermal method also possesses ion exchange property, it may offer a special environment for adsorption of cations, such as basic dyes[5-7] and heavy metal ions[8], through the cation exchange mechanism. On top of that, titanate nanomaterials also has been used in other fields such as photovoltaics, photocatalyst and etc. due to their large surface area However, the questions related to the titanates crystal structure, morphology and other properties are still under discussion[9]. Similar positions and broad peaks of characteristic reflections in XRD

patterns made the titanates structural types is hard to distinguish. Thus, Different crystal structures and compositions have been proposed to describe the TTNT structure, such as bititanate $Na_xH_{2-x}Ti_2O_4(OH)_2$[10], trititanates $H_2Ti_3O_7$[11-15], $H_2Ti_3O_7 \cdot nH_2O$[16], $Na_xH_{2-x}Ti_3O_7$[17,18], tetratitanate $H_2Ti_4O_9 \cdot H_2O$[19,20] and lepidocrocitelike titanate $H_xTi_{2-x/4} \cdot x/4O_4$[21,22]. The main variables in this soft-chemistry process are reaction temperature, and the type of TiO_2 as a raw material. It is well-established that hydrothermal temperature should be within the range of 90-170 °C inasmuch as lower temperatures will impair TiO_2conversion within practical reaction times, whereas higher temperatures may lead to distinct nanoparticle shapes (e.g., nanofibers, belts, or ribbons) other than nanotubes. In this research, the hydrothermal treatment was studied at 100,150, 200 and 250 °C, in order to study the morphology, crystal structure and composition of the synthesised samples. These properties is important to be analysed because it's related to the potential application of the titanate nanostructures materials.

EXPERIMENTAL

2.0 gram of TiO_2 powder precursor (commercial TiO_2 Merck) was dispersed in 10 M NaOH (100 ml) with constant stirring for 30 minutes (500 rpm). Then, the mixture was sonicated in sonicator bath for 30 minutes, after that continue with constant stirring for 30 minutes (500 rpm). Subsequently, the mixture was transferred into Teflon vessel and subjected to hydrothermal treatment at various temperature (100, 150, 200, 250 °C) for 24 hours in autoclave. When the reaction was completed, the white solid precipitate was collected and dispersed into 0.1 M HCL (200 ml) with continuous stirring for 30 minutes (500 rpm) for washing. The washing was repeated by distilled water until the pH of washing solution was 7. The product was subsequently dried at 80 °C for 24 hours in an oven and as-synthesised sample at 100, 150, 200, and 250 °C hydrothermal temperature denoted as HT100, HT150, HT200, and HT250, respectively. The obtained samples were characterized using FTIR, XRD, FESEM and Nitrogen gas adsorption.Perkin Elmer Spectrum 100 FTIR spectrophotometer was used for FTIR spectra analysis from 4000 to 400 cm–1. XRD spectra were recorded at room temperature from 10° to 80° two theta (2θ) using Rigaku Miniflex (II) x-ray diffractometer. FESEM micrographs were captured using JOEL JSM 6360 LA.

RESULTS AND DISCUSSION

Figure 1 shows the FTIR spectra of TiO_2 precursor and as-synthesized sample at 100, 150, 200, and 250 °C hydrothermal temperature denoted as HT100, HT150, HT200, and HT250, respectively. In all studied samples, a broad band has been observed in the range of 3700-2800 cm^{-1} which is referred to the OH stretching mode (TABLE 1). Apart from that, the OH deformation mode at the range 1800-1400 cm^{-1} also has been observed which is corresponding to the presence of the water molecule on the surface of the material[23,24]. The metal-oxygen stretching mode has been detected below 1000 cm^{-1} of wavelength in the samples. A broad peak have been observed due to the Ti-O stretching vibrations mode of surface bridging oxide formed by condensation of adjacent surface hydroxyl group.

XRD analysis was carried out to study the phase structure of hydrothermally synthesized samples at different hydrothermal reaction temperature. For comparison the XRD pattern of TiO_2 precursors (commercial TiO_2 merck) was also included. As can be seen in Figure 2 (a) and (b), the TiO_2 precursor and as-synthesised sample at 100 °C (HT100) shows a series of sharp and narrow peaks assigned to anatase TiO_2 attributed to the existence of highest peaks at ≈25°[23]. Similar XRD pattern of TiO_2 precursor and HT100 suggested the hydrothermal reaction of TiO_2 precursor at low temperature (100 °C) was not happen. This probably because of the TiO_2 is stable compounds especially at low temperature. Meanwhile, for as-synthesised samples at 150 °C (HT150), 200 °C (HT200) and 250 (HT250) hydrothermal treatment, their XRD pattern shows the presence of the peaks at 25.43° and 48.40° (Figure 2 (c)) which is identical as hydrogen trititanate and at 10.86°, 24.83°, and 48.59° belongs to sodium trititanate (Figure 2 (d and e))[25]. These synthesised samples were assigned to trititanate compounds suggesting that the hydrothermal reaction of TiO_2 precursor and NaOH occurs to produce trititanate compounds. In general, the reaction between

Original Research Article

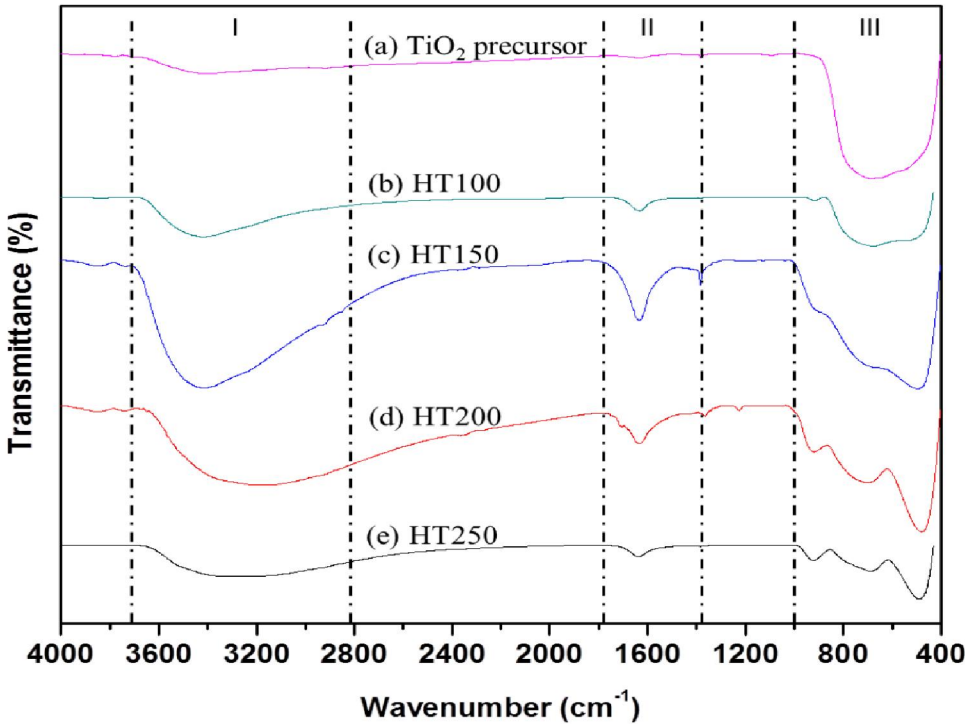

Figure 1: FTIR spectra of (a) TiO_2 precursor, (b) HT100, (c) HT150, (d) HT200, and (e) HT250

TABLE 1: Assignment of FTIR bands for TiO_2 precursor, HT100, HT150, HT200 and HT250

Region	Wavelength (cm^{-1})	Assignment
I	3700 – 2800	OH stretching mode from water molecule
II	1800 – 1400	OH deformation mode from water molecule
III	<1000	Metal-oxygen stretching mode

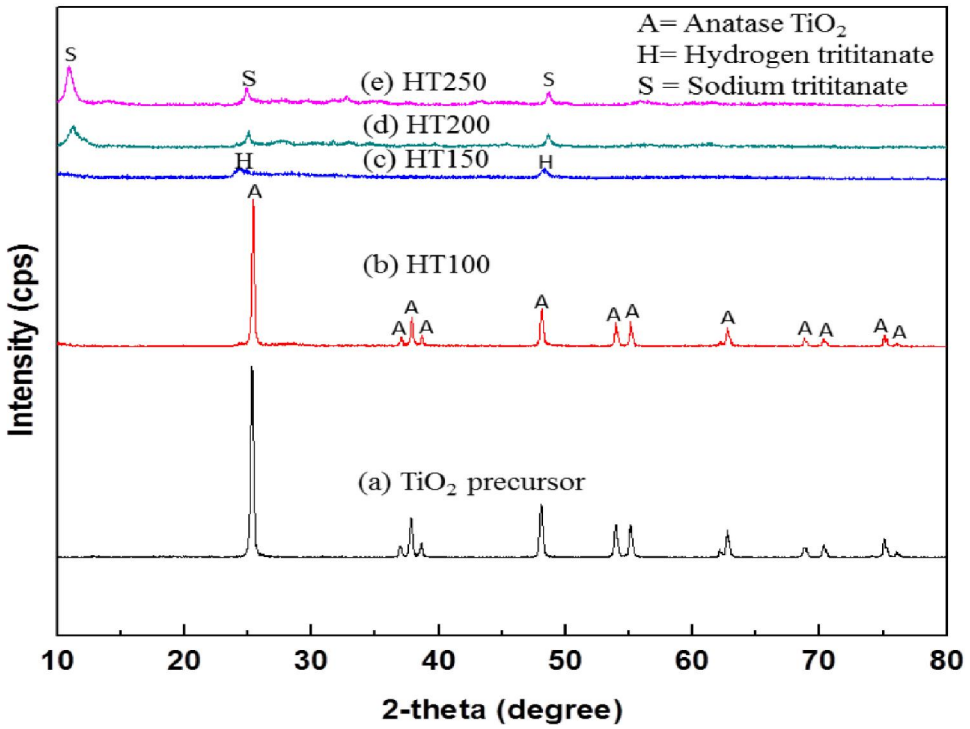

Figure 2: XRD diffractogram of (a) TiO_2 precursor, (b) HT100, (c) HT150, (d) HT200, and (e) HT250

TiO_2 and NaOH produced sodium trititanate and transformed into hydrogen trititanate after washing with HCl. Thus, hydrogen trititanate was obtained at 150 °C. Somehow at 200 and 250 °C, sodium trititanate was produced indicated that sodium trititanate was remained even after washing with HCl. This is probably due to the formation of stable sodium (Na) compound at 200 and 250°C, whereby Na has intercalated in TiO_2 in form of $Na_2Ti_3O_7$. Thus the sodium trititanate was remained even after washing with HCl.

The present of sodium in the sample was proved by EDX analysis as shown in Figure 3(a). While, Figure 3(b) shows the EDX analysis of HT150 sample with an absence of sodium element. This is because at 150 °C, Na^+ cations and the $[TiO_6]$ octahedral layers are held by static interaction in sodium trititanate ($Na_2Ti_3O_7$)[26]. When the larger cations like H^+ were introduced, it can replace the Na^+ cations in the interlayer space of $[TiO_6]$ sheets because the interlayer distance is enlarged and reduces the static interaction. Subsequentlly, the Na^+ was totally exchanged with larger cation of H^+ during HCl washing, to form hydrogen trititanate ($H_2Ti_3O_7$). Therefore, no sodium element was detected in EDX results for HT150 sample.

The morphology of the as-synthesized samples at different hydrothermal temperature and TiO_2 precursors has been studied using FESEM. From the micrograph in Figure 4(a), TiO_2 precursor possessed irregular shape particles with the diameter within 200 – 300 nm. Similar morphology was observed for HT100 sample (Figure 4(b)). This finding recommended that no reaction between TiO_2 and NaOH at 100°C hydrothermal treatment. Interestingly, at 150 °C (HT150) fibrous-like structure was viewed as shown in Figure 4(c). It could be expected that TiO_2 particles reacted with OH^- (from NaOH) to form nanosheet at the initial stage of hydrothermal treatment, and then turned to nanofibers at 150 °C. The diameters of fibers are within 25 – 30 nm with several hundred nanometers in length and attached to each other to form raft-like structures. Meanwhile, rods-like particles are formed when the hydrothermal treatment was done at 200 and 250 °C, respectively (Figure 4(d) and (e). The formation of rod-like particles because at higher hydrothermal treatment, initial nucleation was accelerated thus resulted in rapid growth of particles. Due to the rapid growth of particles, the particles tend to form the layered structures. Then, the layered become thicker and finally rolling up into rods. The diameter of rod-like particles was found to be 250 – 300 nm.

As shown in TABLE 2, the surface area of commercial TiO_2 precursor powder was only 10.07 m^2/g. Nevertheless the surface area of the samples was increased after hydrothermal treatment. At 100°C hydrothermal treatment (HT100), the surface area was found to be 146.74 m^2/g. Meanwhile, HT150 which is the sample prepared at 150°C hydrothermal treatment possessed the largest surface area (320.51 m^2/g). It was believed that the inner and outer surfaces of the fibrous-like structure are the major reason for the increase in surface area. On the other hand, the surface area of as-synthesized sample at 200 °C (HT200) is 117.51 m^2/g, smaller than HT150 due to the presence of rods-like structure instead of fibrous-like TiO_2 structure. This rods-like TiO_2 material agglomerate at higher temperature, therefore the surface area of HT250 sample was found to be only 28.15 m^2/g since this

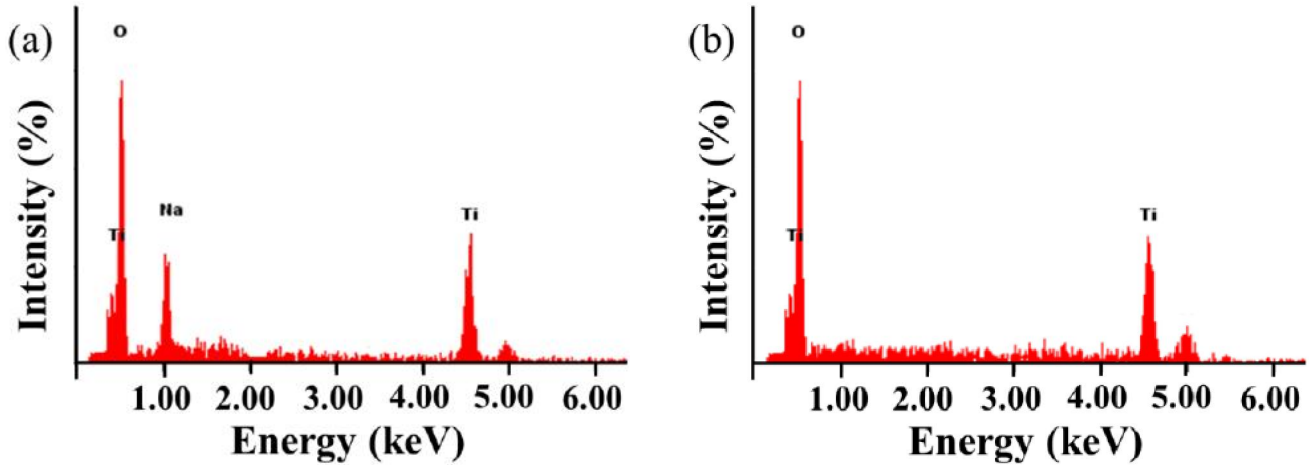

Figure 3: EDX spectra of (a) HT200 and (b) HT150

Original Research Article

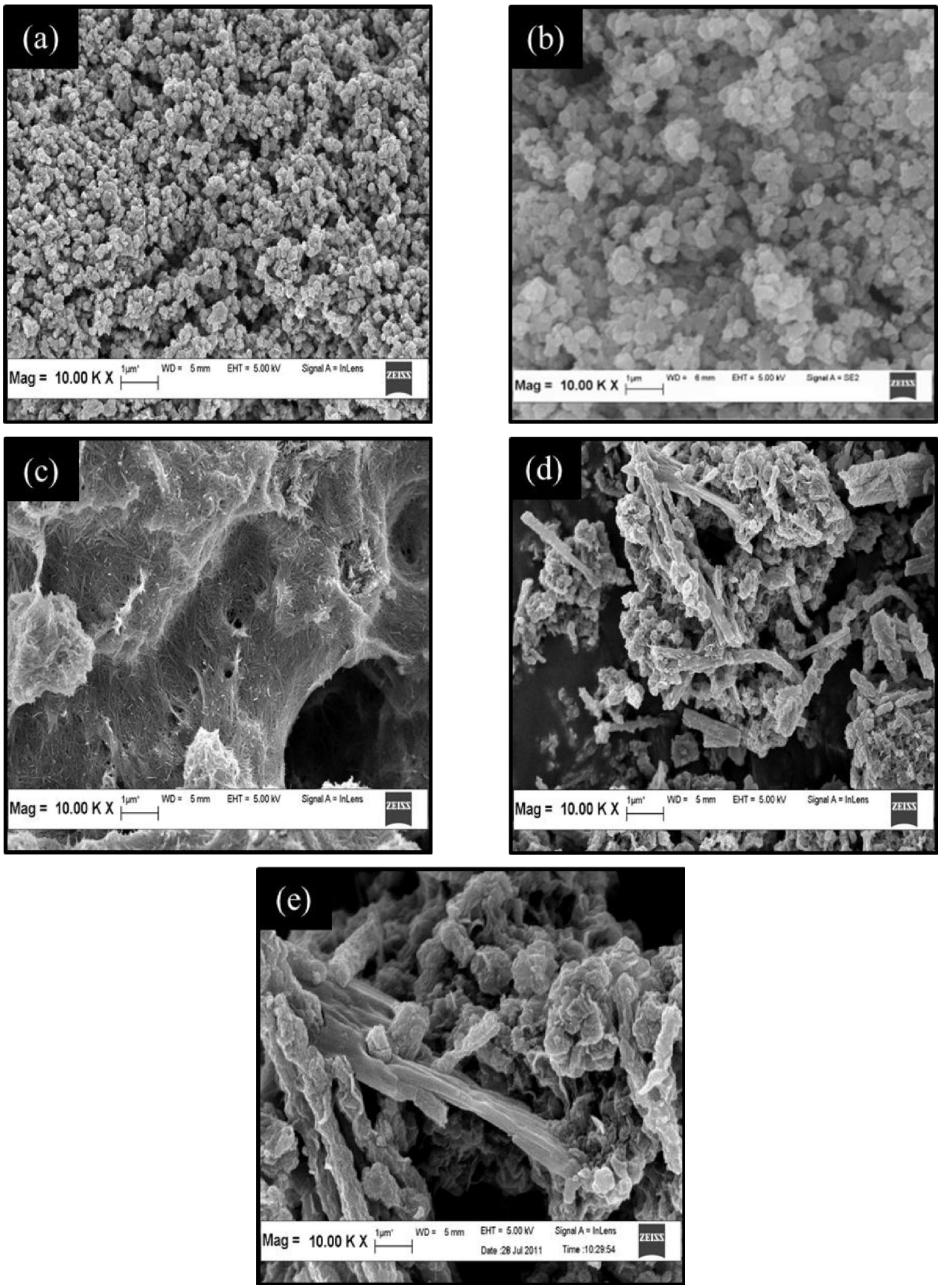

Figure 4: FESEM micrographs of (a) TiO_2 precursor, (b) HT100, (c) HT150, (d) HT200, and (e) HT250

sample was synthesized at highest hydrothermal temperature studied (250 °C). Similar trend was observed for pore volume of the prepared samples (TABLE 2). Larger surface area and high pore volume of the samples will provide more active sites, thus it was expected to be a good adsorbent materials.

Figure 5 show the N_2 adsorption-desorption isotherm plot of the TiO_2 precursor and as-synthesized samples at different hydrothermal temperature treatment. The isotherm for all studied samples exhibits a typical IV-like isotherm with H3 hysteresis according to IUPAC classification[27] (TABLE 3). The types of isotherms have often been identified with specific pore structures. Type IV isotherms appearing in the multilayer range of physisorption isotherms is usually associated with capillary condensation in mesopore structures. Generally, mesoporous structures are encountered with materials having pores in the general range of 2 to 50 nm. As presented in TABLE 2, the pore sizes of the synthesized samples are between 11.29 to 16.32 nm, which is in the mesopore range suggesting very narrow distributions of the mesopore dimensions. Furthermore, the type H3 hysteresis which represents slit shaped pores was in good agreement with the FESEM results obtained.

CELL PROLIFERATION

In vitro wound healing performance for all of the studied samples were assessed for cell viability using 3T3 mouse fibroblast cells at different time interval from 24 h to 48 h and 72 h. The fluorescence images of the cells were shown in Figure 10. The cell spreading gradually as the time increased from 24 h to 48 h and 72 h for all studied films as well as for control sample. However, after 72 h, the cell was not fully spread for GG film and control sample suggesting that neat GG was not helping much for cell growth. On the other, as the time increased up to 72 h, the cells spread significantly for GG + TiO2-NTs (1 w/w %), GG + TiO2-NTs (5 w/ w %) GG + TiO2-NTs (10 w/w %), and GG + TiO2-NTs (15 w/ w %) films. Especially for GG + TiO2-NTs (10 w/w %) film, the cell growth extremely healthy and fully spread after 3 days of culture, recommending that TiO_2 nanotubes was able to promote the cell growth. Previously, nanotubes of smaller diameters 30 nm have been reported to support cell adhesion and spreading due to the larger area density of highly curved nanotube edges[50]. On top of that, small diameter of TiO_2 nanotube surface provides the optimum length scale for integrin clustering and focal contact formation, inducing cell proliferation, migration, and differentiation at a highest rate[51]. However, the cell was reduced and no migration was observed after 3 days for GG + TiO2-NTs (20 w/ w %) films suggesting that TiO2-NTs at higher concentration show toxicity effect. This finding was confirmed further by cell proliferation analysis.

As shown in Figure 11, the number of cell for GG + TiO2-NTs films was increased gradually until day 3 except for GG + TiO2-NTs (20 w/w %) films. The number of cell for GG + TiO2-NTs (1 w/w %), GG + TiO2-NTs (5 w/w %), GG + TiO2-NTs (10 w/w %) and GG + TiO2-NTs (15 w/w %) were ~163,511 cells/ well, ~216, 844 cells/well, ~390, 289 cells/well, and ~333, 400 cells/well, respectively. Meanwhile, for GG + TiO2-NTs (20 w/w %) the number of cell was found to be only ~106, 733 cells/well, which is much lower than pure GG films (~126,733 cells/well) and control sample (~123, 844 cells/well). As reported earlier, TiO2-NTs shows toxicity effect at high concentrations (20 w/w %), therefore GG + TiO2-NTs (20 w/w %) gave the lowest cell number after 3 days. According to the Trojan-horse theory, the metal ions leaching from the nanostructured can enter the fibroblast cells and make

TABLE 2: Surface area, pore size and pore volume of TiO_2 precursor, HT100, HT150, HT200, and HT250

Samples	Surface area (m^2/g)	Pore size (nm)	Pore volume (cm^3/g)
TiO_2 precursor	10.07	12.36	0.03
HT100	146.74	11.29	0.43
HT150	320.51	14.93	1.36
HT200	117.51	16.32	0.53
HT250	28.15	14.90	0.09

TABLE 3: Types of isotherms, hysteresis, pores and shape of pores of TiO_2 precursor, HT100, HT150, HT200, and HT250

Samples	Type of isotherms	Type of hysteresis	Type of pores	Shape of pores
TiO_2 precursor	IV	H3	Mesopore	Slit shaped pores
HT100	IV	H3	Mesopore	Slit shaped pores
HT150	IV	H3	Mesopore	Slit shaped pores
HT200	IV	H3	Mesopore	Slit shaped pores
HT250	IV	H3	Mesopore	Slit shaped pores

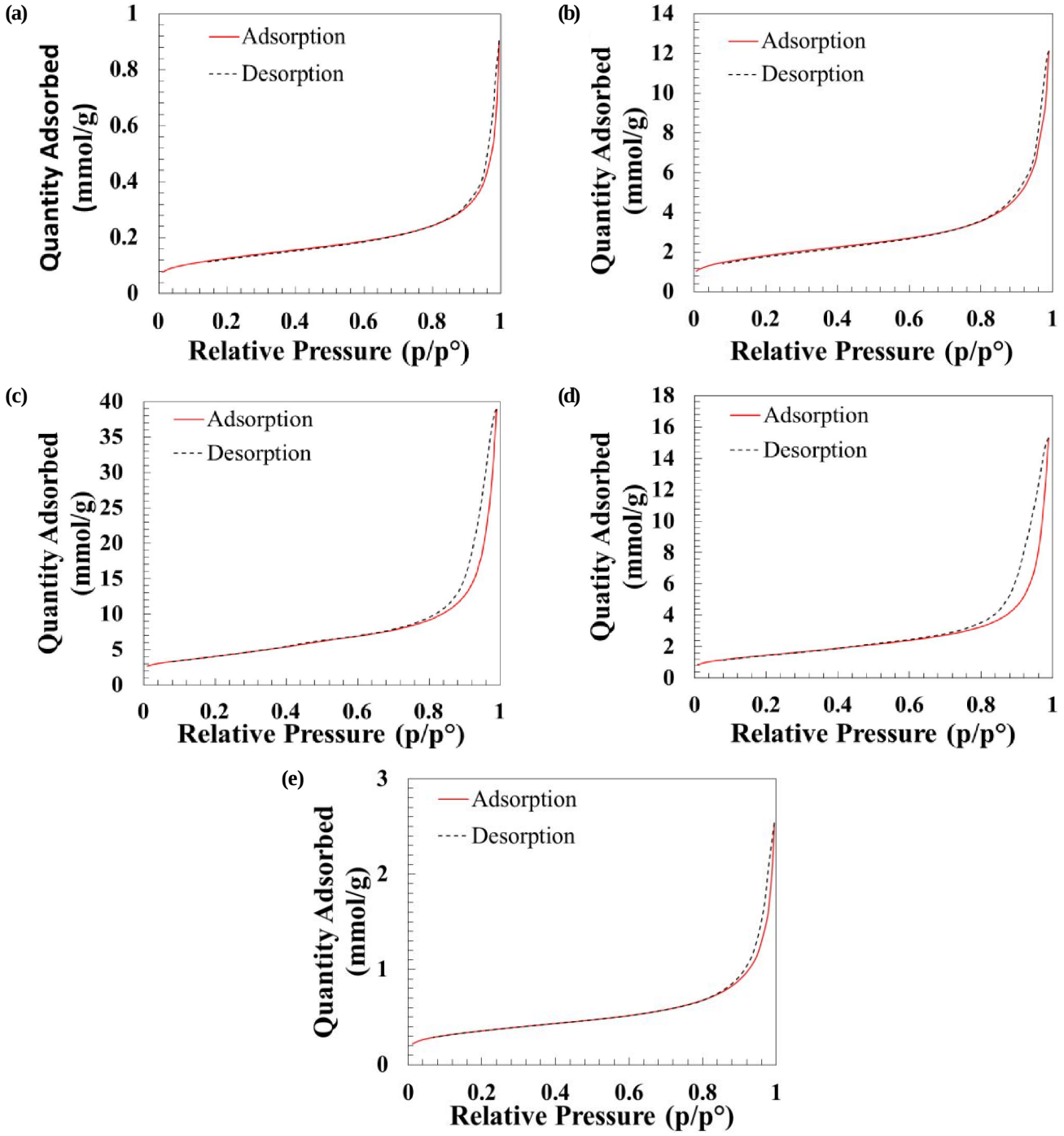

Figure 5: Nitrogen adsorption-desorption isotherms (a) TiO_2 precursor, (b) HT100, (c) HT150, (d) HT200, and (e) HT250

them toxic at higher concentration. Among the GG + TiO2-NTs nanocomposite films, GG + TiO2-NTs (10 w/w %) film gave the highest cell number after 24 h and 48 h incubation period. After 3 days, the number of cell is ~390, 289 cells/well, showing that incorporating TiO2-NTs at 10 w/w % promoted 3T3 mouse fibroblast cell proliferation on the GG films. These findings proved that the GG + TiO2-NTs film is favourable for cell adhesion, biocompatible and non-toxic at suitable concentration.

Only two samples was selected for TG analysis which are as-synthesised samples at 150 (HT150) and 200°C (HT200). This is because no reaction was observed for HT100 sample, while HT250 sample similar to HT200. The thermograms (TG) obtained for HT150 and HT200 were shown Figure 6. Similar TG

curves were observed for both samples, which are showing rapid decreased in mass starting at room temperature until 700 °C. Total mass loss is about 15% and 22%, respectively. Generally, the weight loss between room temperature till 100°C is due to the removal of adsorbed water from the surface. When the temperature is further increased up to 300°C, the removal of the intercalated water molecules included dissociated molecular H_2O, physisorbed molecular H_2O and chemisorbed molecular H_2O are occurred. Subsequently, a small of weight loss in the region of 300-700°C, is probably due to the transformation of crystal structure of trititanate into titania (TiO_2). In order to study the transition of trititanate into titania, samples was further studied at different calcination temperature which are at 300, 400, 500, and 700 ° C.

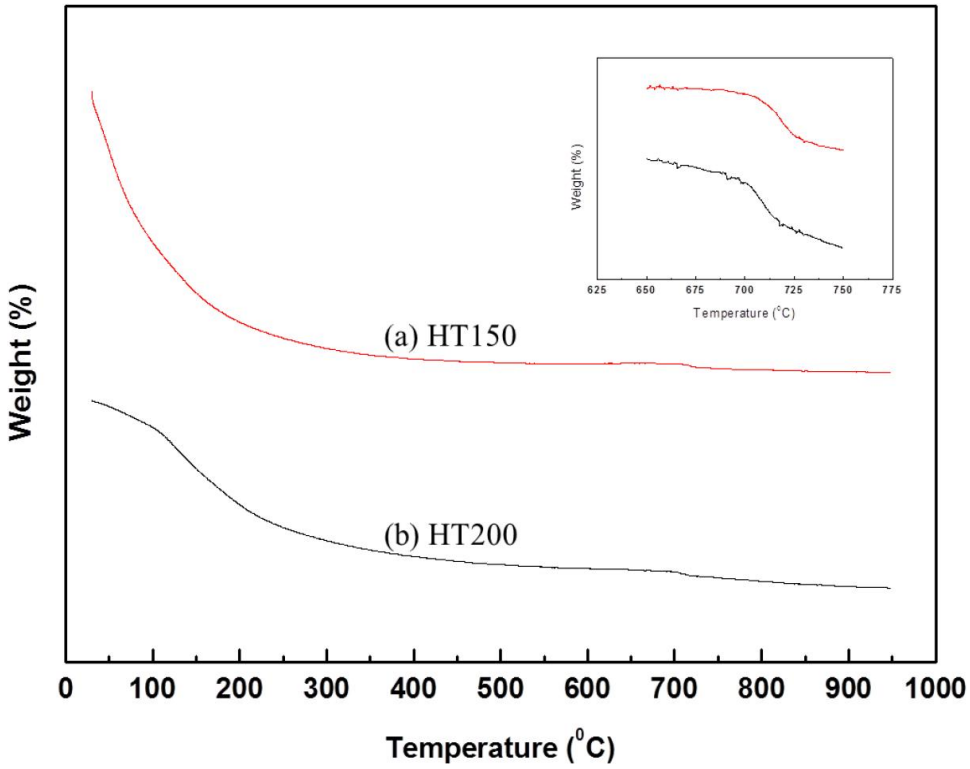

Figure 6: TGA themograms of (a) HT150 and (b) HT200

CONCLUSION

Titanate nanostructured materials were successfully synthesized using simple hydrothermal method at different temperature. At low hydrothermal treatment temperature, 100 °C (HT100) no reaction was occurred, thus similar properties of the as-synthesised material with TiO_2 precursors were observed. At 150°C hydrothermal treatment (HT150), trititanate compounds was produced corresponding to hydrogen trititanate nanofibrous, while sodium trititanate nanorods was obtained at 200°C (HT200) and 250°C (HT250). Highest surface area of hydrogen trititanate nanofibrous recommended that materials has a great potential to be used as adsorbent.

ACKNOWLEDGEMENT

The authors are grateful to Universiti Malaysia Terengganu (UMT) for providing the facilities to carry out this project and Ministry of Higher Education. Malaysia for the financial support vote (FRGS/1/2019/STG07/UMT/02/2)

REFERENCES

[1] T.Kasuga, M.Hiramatsu, A.Hoson, T.Sekino, K.Niihara; Formation of titanium oxide nanotube. Langmuir, **14**, 3160-3163 **(1998)**.

[2] D.S.Seo, J.K.Lee, H.Kim; Preparation of nanotube-shaped TiO_2 powder. J.Cryst.Growth, **229**, 428-432 **(2001)**.

[3] T.Kasuga; Formation of titanium oxide nanotubes using chemical treatments and their characteristic properties. Thin.Solid Films, **496**, 141-145 **(2006)**.

[4] J.Yu, H.Yu, B.Cheng, X.Zhao, Q.Zhang; Preparation and photocatalytic activity of mesoporousanatase TiO2 nanofibers by a hydrothermal method. J.PhotochemPhotobiol.A, **182**, 121- **(2006)**.

[5] C.K.Lee, S.S.Liu, L.C.Juang, *et al.*; Application of titanate nanotubes for dyes adsorptive removal from aqueous solution. J.Hazard.Mater., **148**, 756-760 **(2007)**.

[6] C.K.Lee, K.S.Lin, C.F.Wu, M.D.Lyu, C.C.Lo; Effects of synthesis temperature on the micro-structures and basic dyes adsorption of titanate nanotubes. J.Hazard.Mater., **150**, 494-503 **(2008)**.

[7] C.K.Lee, C.C.Wang, L.C.Juang, *et al.*; Effects of sodium content on the microstructures and basic dye cation exchange of titanate nanotubes. Colloid Surf.A PhysicochemEng.Aspects, **317**, 164-173 **(2008)**.

[8] S.S.Liu, C.K.Lee, H.C.Chen, C.C.Wang, L.C.Juang; Application of titanate nanotubes for Cu(II) ions adsorptive removal from aqueous solution. ChemEng.J., **147**, 188-193 **(2009)**.

[9] E.Morgado Jr., P.M.Jardim, B.A.Marinkovic, F.C.Rizzo, M.A.S.de Abreu, J.L.Zotin, A.S.Araujo; Nanotechnology, **18**, 495710, 10pp **(2007)**.

[10] M.Paulose, K.Shankar, O.K.Varghese, G.K.Mor, C.A.Grimes; Application of highly-ordered TiO2 nanotube-arrays in heterojunction dye-sensitized solar cells. J.Phys.D-ApplPhys., **39**, 2498-2503 **(2006)**.

[11] X.B.Chen, S.S.Mao; Titanium dioxide nano-materials: Synthesis, properties, modifications, and applications. Chem.Rev., **107**, 2891-2959 **(2007)**.

[12] H.U.Ou, S.L.Lo; Review of titania nanotubes synthesized via the hydrothermal treatment: Fabrication, modification, and application. Sep. PurifTechnol., **58**, 179-191 **(2007)**.

[13] V.Štengl, S.Bakardjieva, J.Šubrt, *et al.*; Sodium titanate nanorods: Preparation, microstructure characterization and photocatalytic activity. ApplCatal.B Environ., **63**, 20-30 **(2006)**.

[14] J.M.Wu; Photodegradation of rhodamine B in water assisted by titaniananorod thin films subjected to various thermal treatments. Environ.SciTechnol., **41**, 1723-1728 **(2007)**.

[15] M.Hodos, E.Horvath, H.Haspel, A.Kukovecz, Z.Konya, I.Kiricsi; Photo sensitization of ion-exchangeable titanate nanotubes by CdS nano-particles. ChemPhysLett., **399**, 512-515 **(2004)**.

[16] J.C.Xu, M.Lu, X.Y.Guo, H.L.Li; Zinc ions surface-doped titanium dioxide nanotubes and its photocatalysis activity for degradation of methyl orange in water. J.MolCatal.A Chem., **226**, 123-127 **(2005)**.

[17] Y.X.Yu, D.S.Xu; Single-crystalline TiO2 nanorods: Highly active and easily recycled photocatalysts. ApplCatal.B Environ., **73**, 166-171 **(2007)**.

[18] H.Yu, J.Yu, B.Cheng, J.Lin; Synthesis, characterization and photocatalytic activity of mesoporoustitanianano rod/titanate nanotube composites. J.Hazard.Mater., **147**, 581-587 **(2007)**.

[19] L.R.Hou, C.Z.Yuan, Y.Peng; Synthesis and photocatalytic property of SnO2/TiO2 nanotubes composites. J.Hazard.Mater., **139**, 310-315 **(2007)**.

[20] V.Idakiev, Z.Y.Yuan, T.Tabakova, B.L.Su; Titanium oxide nanotubes as supports of nano-sized gold catalysts for low temperature water-gas shift reaction. ApplCatal.A Gen., **281**, 149-155 **(2005)**.

[21] D.V.Bavykin, A.A.Lapkin, P.K.Plucinski, L.Torrente-Murciano, J.M.Friedrich, F.C.Walsh; Deposition of Pt, Pd, Ru and Au on the surface of titanate nanotubes. Top Catal., **39**, 151-160 **(2006)**.

[22] D.V.Bavykin, J.M.Friedrich, F.C.Walsh; Protonated titanates and TiO2 nanostructured materials: Synthesis, properties, and applications. Adv.Mater., **18**, 2807-2824 **(2006)**.

[23] M.H.Razali, M.Ahmad-Fauzi, A.R.Mohamed, S.Sreekantan; Physical Properties Study of TiO2 Nanoparticle Synthesis Via Hydrothermal Method using TiO_2 Microparticles as Precursor. Advanced Materials Research, **772**, 365-370 **(2013)**.

[24] S.Subhapriya, P.Gomathipriya; Green synthesis of titanium dioxide (TiO_2) nanoparticles by Trigonella foenum-graecum extract and its antimicrobial properties. Microbial Pathogenesis, **116**, 215-220 **(2018)**.

[25] M.H.Razali, A.-F.Mohd Noor, A.R.Mohamed, S.Sreekantan; Morphological and Structural Studies of Titanate and Titania Nanostructured Materials Obtained after Heat Treatments of Hydrothermally Produced Layered Titanate. Journal of Nanomaterials, **2012**, 10 **(2012)**.

[26] C.Xiaobo, S.M.Samuel; Titanium Dioxide Nanomaterials: Synthesis, Properties, Modifications, and Applications. Chemical Review, **107**, 2891-2959 **(2007)**.

[27] M.Kruk, M.Jaroniec; Gas adsorption characterization of ordered organic – inorganic nanocomposite materials. Chemistry of Materials, **13(10)**, 3169-3183 **(2001)**.